# Integration of UAV Photogrammetry and GIS in High-Resolution Topographic Mapping of Kedungsari Village, Temayang Subdistrict

### Mrabawani Insan Rendra\*, Ahmad Adivin, Arya Kusuma Hadi

Civil Engineering Study Program, Faculty of Science and Engineering, Bojonegoro University

\*Email: m.insanrendra@gmail.com

DOI: https://doi.org/10.31284/j.jtm.2025.v6i2.7849

Received June 14th 2025; Received in revised July 15th 2025; Accepted July 25th 2025; Available online July

31st 2025

Copyright: ©2025 Tulus Doan, Evan Nugraha, Oviyan Patra License URL: https://creativecommons.org/licenses/by-sa/4.0

#### Abstract

This study aims to acquire photogrammetric data for the purpose of generating a slope map of Kedungsari Village. Aerial imagery was captured using a drone flown at a specific altitude with optimal overlap and sidelap settings. To enhance positional accuracy, ground control points (GCP) were established and surveyed using the static method of Geodetic GPS. The data processing workflow involved photo alignment, georeferencing, dense point cloud generation, point cloud classification, digital elevation model (DEM) creation, and orthomosaic generation. The slope map was derived from a Digital Terrain Model (DTM), which was classified into several categories based on slope gradient. The resulting map is expected to serve as a reference for landslide susceptibility analysis and land-use planning.

Keywords: DEM, Drone, Photogrammetry, GCP, Slope Map

### Abstrak

Penelitian ini bertujuan untuk memperoleh data fotogrametri guna menyusun peta kemiringan lahan di Desa Kedungsari. Akuisisi foto udara dilakukan menggunakan drone pada ketinggian tertentu dengan pengaturan overlap dan sidelap yang optimal. Untuk meningkatkan akurasi, titik kontrol dipasang dan diamati menggunakan GPS Geodetik metode statik. Proses pengolahan data mencakup photo alignment, georeferencing, pembuatan dense cloud, klasifikasi point cloud, pembuatan DEM, dan orthomosaic. Peta kemiringan lahan dihasilkan dari Digital Terrain Model (DTM) yang diklasifikasikan ke dalam beberapa kategori berdasarkan kemiringan lereng. Hasil pemetaan ini diharapkan dapat digunakan sebagai dasar dalam analisis kerawanan longsor dan perencanaan tata guna lahan.

Kata Kunci: DEM, Drone, Fotogrametri, GCP, Peta Kemiringan

### 1. Introduction

Land slope is one of the main factors in topographic analysis that greatly influences the level of vulnerability of an area to geological disasters, especially landslides. Areas with steep slopes tend to have low soil stability, making it easier to experience soil mass movement during high rainfall, weathering, or due to uncontrolled land use change. Therefore, land slope mapping is an important first step in disaster mitigation efforts and risk-based spatial planning.

The use of unmanned aerial vehicles (UAVs) as the main tool in remote sensing technology has been applied in various scientific fields to support research, environmental monitoring, agriculture, and analysis of geospatial conditions[1], [2]. *Unmanned Aerial Vehicles* (UAVs) equipped with digital cameras, when combined with a photogrammetric image processing technique called *Structure from Motion* (SfM), have become an effective technological solution for obtaining high-precision points in

\* Mrabawani Insan Rendra ISSN: 2721-1878 | DOI: 10.31284/j.jtm.2025.v6i2.7849

the preparation of *Digital Terrain Models* (DTM) with high spatial resolution[3], [4]. This technology provides high spatial resolution as well as advantages in terms of operational flexibility when compared to conventional methods such as satellite imagery and ground surveys. The development of mapping technology using Unmanned Aerial Vehicles (UAVs) or drones has opened up great opportunities for efficient and detailed topographic mapping. The utilization of UAVs with photogrammetric methods allows accurate and efficient spatial data collection, so as to produce topographic maps and earth surface models with a high level of detail that are useful in various applications such as land mapping, spatial planning, and environmental analysis[5], [6]. Through the photogrammetric method, drones are able to produce high-resolution aerial imagery which is then processed into a digital elevation model (DEM). Digital Elevation Model (DEM) is a digital representation of the contours of the earth's surface that records the elevation variations of an area in the form of a grid or matrix of elevation values. DEMs present topographic information numerically and are widely used in various geospatial applications such as slope mapping, hydrological analysis, spatial planning, flood modeling, as well as monitoring land morphological changes[7], [8]. This model allows land slope analysis to be done accurately and thoroughly, especially in areas that are difficult to reach with traditional survey methods. In order for the mapping results to have a high level of accuracy, drone flight planning is carried out systematically by considering flight paths and the use of ground control points (GCP). Ground Control Points (GCP) are reference points on the earth's surface whose coordinates are known precisely through geodetic measurements, such as differential GPS. These points are used as references in the process of geometric correction and calibration of image data in remote sensing, in order to improve the spatial accuracy of mapping results or photogrammetric models[9], [10], [11]. The image data obtained is then processed through technical stages such as camera orientation, three-dimensional reconstruction, and elevation data extraction. The resulting slope map is an important basis in identifying landslide potential and supporting decision-making in land management.

Kedungsari Village rests in the hilly heart of Temayang Sub-district, Bojonegoro Regency, where rise and drop trace an uneven line across the landscape. That very topography invites trouble once rain sets in, sliding loose earth into gamble. A clear slope map could reveal weak points and guide decisions that leave the village sturdier next season. The present inquiry therefore flies a UAV over the settlement, stitches the frames into a contour grid, then tallies degrees of pitch against the threshold where failure typically begins.

# 2. Methods

Data collection in this study was carried out by utilizing *Unmanned Aerial Vehicle* (UAV) technology to obtain detailed and accurate topographic information[1], [12], [13]. During the field survey, researchers acquired surface-elevation information by conducting a detailed topographic map of the study corridor. A differential-GPS unit supplemented the ground work, tightening the spatial precision of the final plot.

Topographic data acquisition relied on a photogrammetric workflow fueled by UAV-derived imagery, a method chosen for its capacity to render elevation distribution and contour details with millimeter-level precision. In this context, photogrammetry denotes a geometric mapping technique that synchronizes overlapping aerial photographs to create an accurate three-dimensional representation of terrestrial features. The images themselves are captured at a predetermined altitude by the unmanned aerial system, ensuring sufficient overlap and parallax for subsequent dense point-cloud generation[14]. Meanwhile, according to[15] photogrammetry is one of the efficient surveying and mapping methods. Photogrammetric surveying, conducted from a modest altitude, can blanket extensive tracts of landscape almost in a single sweep and still yield a striking degree of detail. Such photo mosaics, usually printed or displayed at large scales, prove invaluable for preliminary planning decisions. Once the images sit in a GIS environment, routine spatial-analysis routines translate them into profiles of land cover, slope, and drainage by exploiting elevation, reflective signature, and positional metadata. Typical data hygiene chores at this stage include fine-tuning orientation via geometric corrections, overlaying precise GPS vectors, and sculpting relief features in

the form of digital elevation models and traditional contour sets. *Digital Elevation Model* (DEM) is a representation that describes the height of each point on the image that has gone through processing[14]. Once the individual data sets have been cleaned and harmonized, they are uploaded into a geographic information system, where they coalesce into a composite land-slope map. That visual product captures every rise and run across Kedungsari Village and in turn supplies a platform for gauging the communities exposure to geological hazards, chief among them slope-driven landslides.

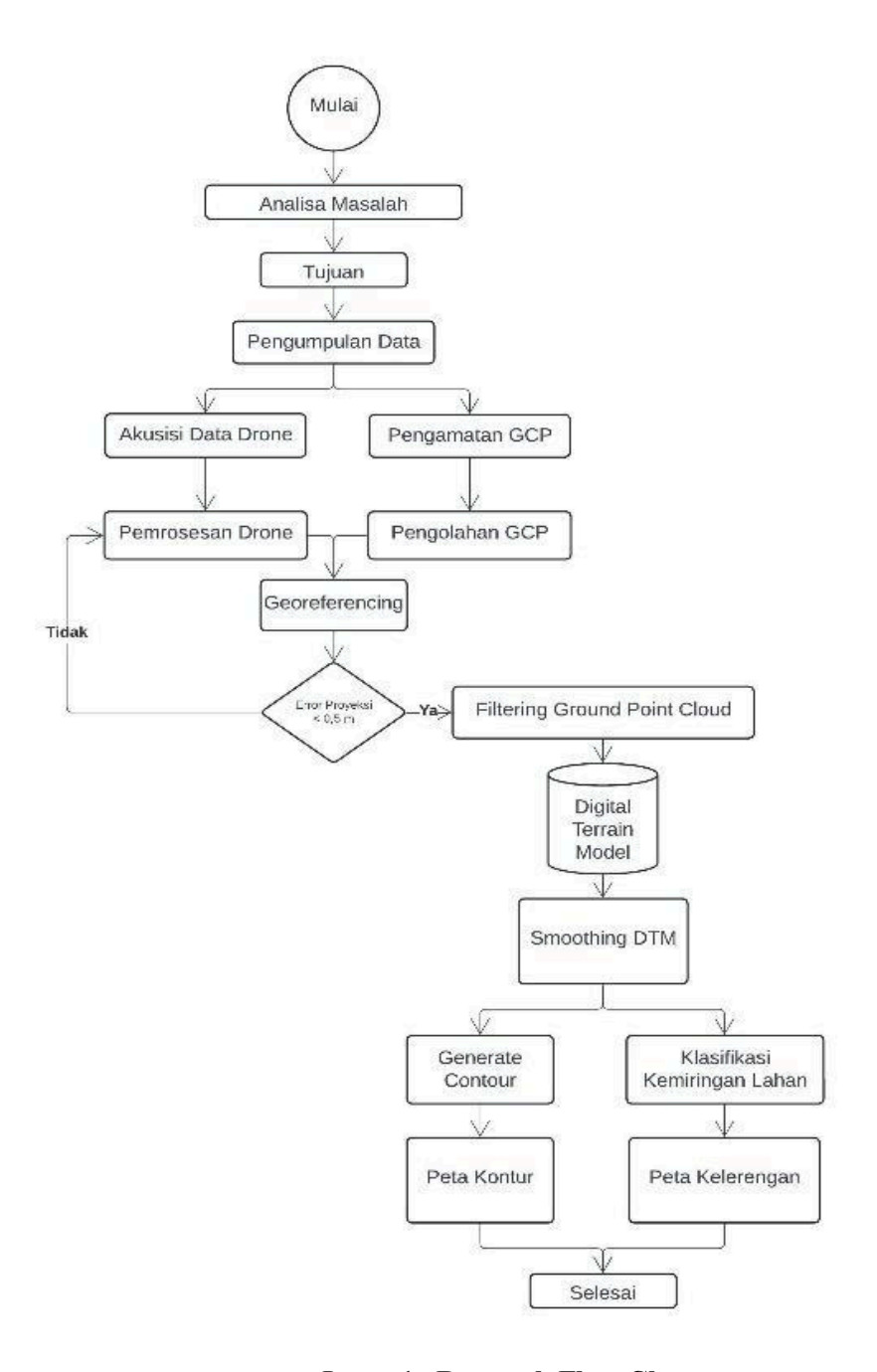


**Image1** . Research Flow Chart

In the present investigation, data gathering unfolded along two distinct but complementary pathways. Remote sensing crews launched unmanned aircraft along carefully choreographed flight corridors, capturing high-resolution images that would map the landscape from above. These aerial

frames were intended to sketch a broad topographic portrait of the site. Simultaneously, surveyors paced the ground, registering a network of Ground Control Points with dual-frequency geodetic receivers or handheld total stations. Each point acted as a terrestrial anchor, pinning the airborne photographs to real-world coordinates and tightening their spatial fidelity. Once stacked and corrected, the dual datasets served as raw material for subsequent processing, ultimately yielding an accurate relief model of the region.

Once the field campaign was completed and every megabyte of imagery had been secured, the workflow advanced to data processing. The first step, accomplished with dedicated photogrammetric software, tidied the drone photographs and registered them to one another. Out of that choreographed sequence a dense three-dimensional point cloud emerged, laying the groundwork for a detailed surface model.

Secondly, *Ground Control Points* (GCP) data obtained through GPS measurements were calibrated and adjusted[16]. Photogrammetric surveys often suffer from persistent positional drift, a defect that undermines the utility of the final elevation models. Rectifying that drift depends on rigorous georeferencing; only then will the resulting maps mirror the topography surveyed in the field. The next logical move in the workflow simply joins the drone-derived images with the field-measured ground control points. At this juncture matching the airborne perspective to known terrestrial coordinates is the primary goal, a step that firms up the entire spatial framework of the project.

Following the georeferencing step, analysts typically gauge horizontal and vertical position error by direct comparison with a reliable reference dataset. A margin of 0.15 meters usually serves as the practical tolerance; measurements that fall within that window are cleared for advance processing. Conversely, observations that breach the threshold trigger a renewed adjustment of the georeferencing parameters in hopes of sharpening overall spatial accuracy. When the dataset finally qualifies, point-cloud filtering is undertaken to isolate returns from the bare ground, discarding reflections from vegetation, buildings, or parked vehicles. The cleaned subset then becomes the foundation for constructing a digital terrain model, ensuring that the resultant DTM closely mirrors the true Earth's surface.

After filtering is complete, a DTM is created which is a digital representation of the ground surface without any other objects on it. This classification process aims to produce a set of points that only accurately reflect the ground surface. These points are then used as the basis for creating a *Digital Terrain Model* (DTM)[4], [17], [18] . Elevation and slope measurements are among the most straightforward uses for a Digital Terrain Model, yet practical applications extend far beyond that initial utility. Even a freshly derived DTM is rarely pristine; random artifacts and topographic jitter often mar the surface grid, so some form of smoothing or filtering is typically the first step toward a more plausible representation of real-world relief. Subsequent post-processing tasks then convert the cleaned model into familiar deliverables-contour plots that trace elevation bands across a landscape and land-slope classification maps that designate which slopes verge on gentle and which climb into sheer gradients.

Table 1 . Software and Hardware used

Category	Device Name	Function
	JOUAV CW-007 Fix Wing UAV	Rides for aerial photo shooting
	Dell Latitude 7490 Laptop (Intel Core i5 Gen 6, 16GB RAM)	Remote drone control and report writing
Hardware	HI-Target V60 Geodetic GPS	GCP and ICP measurements
панимане	Acer Nitro 5 Laptop (AMD Ryzen 5, 16GB RAM, RTX 4060Ti	Processing of acquired data
	8GB VGA)	
-	Marker (20x100 cm tarpaulin, 20 pieces)	Marker for control points
	Google Earth	Create a flying area and control point plan
	JOUAV CW Commander	Create a flight path plan and control the
		drone
Software	Hi Target Geomatics Office	GPS data processing
	Microsoft Office Word and Excel	Accuracy test data processing and report
		writing
	Agisoft Metashape 2.2.0	Drone data processing
	ArcGIS 10.8	Mapping data processing

After photo acquisition, the acquired data is processed through several stages. The first process is *photo alignment* and *georeferencing* with GCPs to align the image with precise coordinates. Then, *dense cloud*, *Digital Elevation Model* (DEM) and *orthomosaic* were created to obtain a detailed topographic model and orthophoto image with geometric correction.

### 3. Results and Discussion

This research was conducted in Kedungsari Village, Temayang Sub-district, Bojonegoro Regency. The visual description of the research area can be seen in Figure 3.1, which displays the administrative boundaries of Kedungsari Village. This research will focus on making a slope map in Kedungsari Village, Temayang District, Bojonegoro Regency using drone photogrammetry technology.

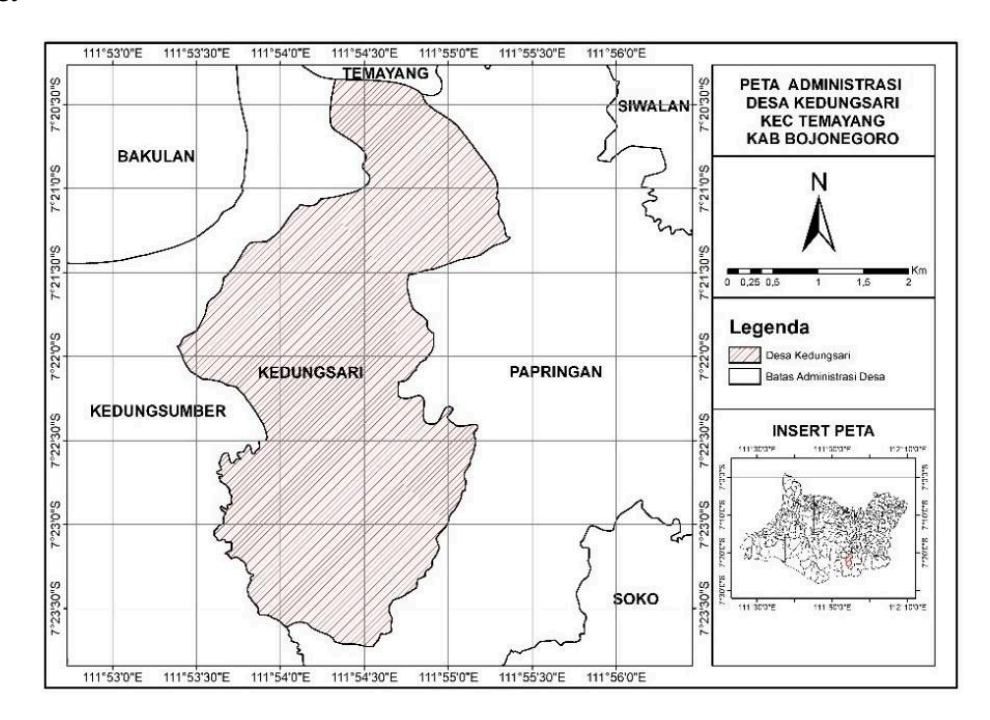
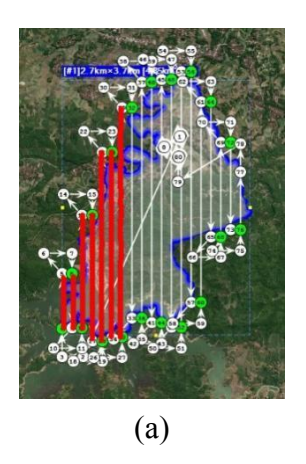
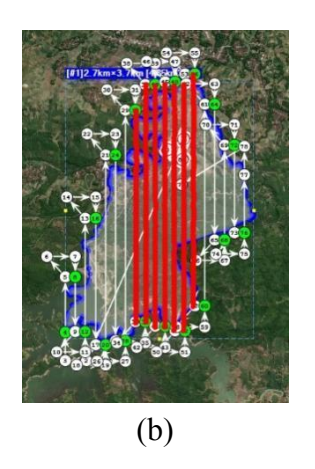


Figure 2. Research Location

### 3.1. Photogrammetric Photo Acquisition for Kedungsari Village Mapping

In this study, the flight path was designed to cover an area of 9 km<sup>2</sup> in Kedungsari Village, with dimensions of 2.8 km x 2.4 km. Due to the limited flying time of the drone, the flight path was divided into three parts, with a total of 17 paths, consisting of:





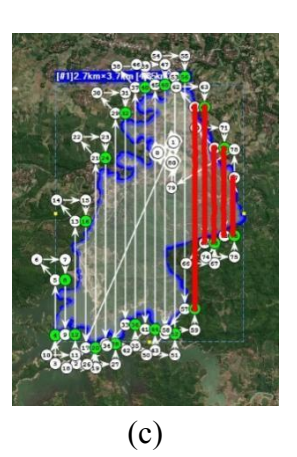


Figure 3. Map of UAV Flight Paths in Kedungsari Village, (a) Line 1 as many as 7 lines, (b) Line 2 as many as 8 lines, (c) Line 3 as many as 2 lines.

Photo acquisition was conducted at an altitude of 550m above sea level, resulting in a Ground Sampling Distance (GSD) of 5 cm. The images were taken using 70% overlap and sidelap, ensuring that the images could be well organized for further processing in mapping.

### 3.2. Results of Control Point Installation and Observation

In this study, the installation of control points was carried out by spreading 20 points throughout the Kedungsari Village area, consisting of 10 *Ground Control Points* (GCP) and 10 *Independent Check Points* (ICP). These points were marked with tarpaulins measuring 1 m x 20 cm, installed in a cross shape for easy recognition in drone image processing.





Installation and Observation of Control Points in Kedungsari Village, (a) Observation of Control Points, (b) Installation of Control Points

Control point observations were made using Geodetic GPS with the static method for 30 minutes per point. The observation data in RINEX format was then converted to 20b using HGO before being processed in the Geospatial Information Agency's Spider Business Center web (http://nrtk.big.go.id/).

**Table 2. GCP Data Processing Results** 

140	ic zi GCI Dutu	Trocessing resu	100
POINT	X	Y	Z
GCP_1_KEDUNGSARI	133783.824	688461.017	57.5514
GCP_2_KEDUNGSARI	135119.764	687934.361	23.5394
GCP 3 KEDUNGSARI	134584.746	687251.058	24.4954

GCP_4_KEDUNGSARI	134162.286	685930.211	115.7163
GCP_5_KEDUNGSARI	135884.3	685529.276	201.4281
GCP_6_KEDUNGSARI	135119.378	686025.62	119.4977
GCP_7_KEDUNGSARI	135899.226	687512.461	52.8061
GCP_8_KEDUNGSARI	135441.125	688465.097	21.41
GCP_9_KEDUNGSARI	133726.55	687309.883	55.8697
GCP_10_KEDUNGSARI	135537.869	686771.972	104.5006

**Table 3. ICP Data Processing Results** 

POINT	X	Y	Z
ICP_1_KEDUNGSARI	134980.679	688437.586	18.4277
ICP_2_KEDUNGSARI	135602.51	687647.842	48.8957
ICP_3_KEDUNGSARI	134539.205	687132.181	31.4735
ICP_4_KEDUNGSARI	134071.388	686186.169	117.1045
ICP_5_KEDUNGSARI	135527.596	685661.924	184.6241
ICP_6_KEDUNGSARI	134935.834	685709.854	152.5909
ICP_7_KEDUNGSARI	135753.618	687306.294	48.5095
ICP_8_KEDUNGSARI	135243.742	688162.051	22.0789
ICP_9_KEDUNGSARI	134008.063	687901.076	78.3924
ICP_10_KEDUNGSARI	135113.35	686567.521	84.4801

The processing results in the form of point coordinates which are then arranged in a table to be used in the drone acquisition data processing process as GCP and ICP.

# 3.3. Aerial Photo Data Processing for Kedungsari Village Mapping

The processing of aerial photography data in this study involved several main stages, including data import, *photo alignment, georeferencing, point cloud processing*, DEM generation, *orthomosaic*, and correction of results using ICP.

# 3.3.1 Import Photo Data and Coordinates

The drone-shot photos and their coordinates were imported into Agisoft for processing. The data from each flight path was combined so that they could be processed simultaneously. The *photo alignment* process is performed to arrange and adjust the photos to form an accurate model. In this study, 1,150 photos were obtained. However, a small area in the form of a reservoir experienced problems in the alignment process due to water reflection, optical distortion, and limited lighting underwater. These constraints did not affect the main results as the research focused on terrestrial topography.

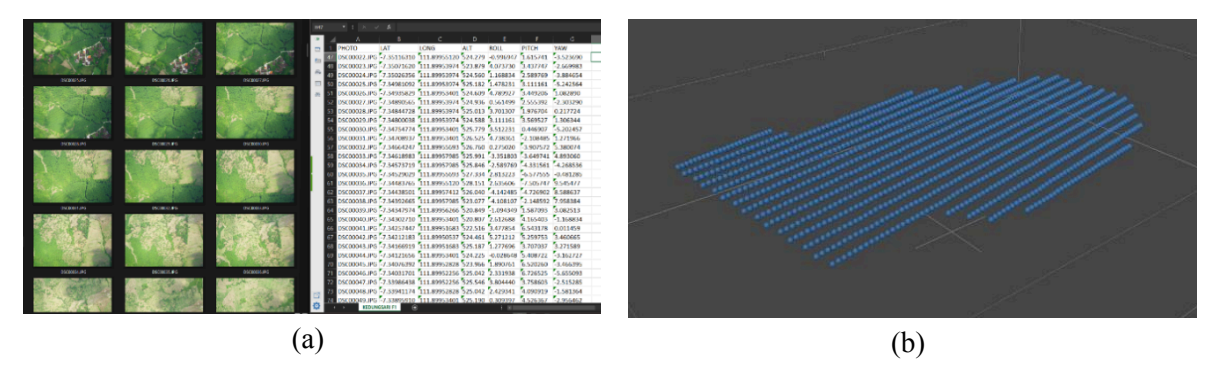


Photo and Coordinate data input,

# (a) Photo Input, (b) Point Coordinates

# 3.3.2 GCP Matching

After *alignment, Ground Control Points* (GCPs) were inserted as markers for *georeferencing* to improve accuracy. The 10 observed GCP points were manually corrected to be close to the reference coordinates.





Figure 6. Georeferencing GCPs

### 3.3.3 Build Dense Cloud and Classify Point Cloud

This stage produces a dense cloud, which is a collection of 3D points that represent the surface of a physical object. Corrections are made based on the confidence level to ensure accuracy. Tahap ini menghasilkan dense cloud berupa himpunan titik 3D yang merepresentasikan permukaan objek fisik secara detail. Proses dilakukan dengan parameter quality = high dan depth filtering = mild. the point density reaches approximately  $\pm 350$  points/m², indicating a high level of spatial resolution suitable for topographic modeling.

The point cloud classification was conducted using a combination of automated and manual methods. The initial classification utilized software algorithms to distinguish objects such as ground, vegetation, and buildings, which was then refined through manual classification based on height thresholding and visual interpretation.

Validation was carried out using orthophotos and the Digital Elevation Model (DEM), without the involvement of ground truth data, in order to ensure the accuracy of the DTM in representing the actual ground surface.

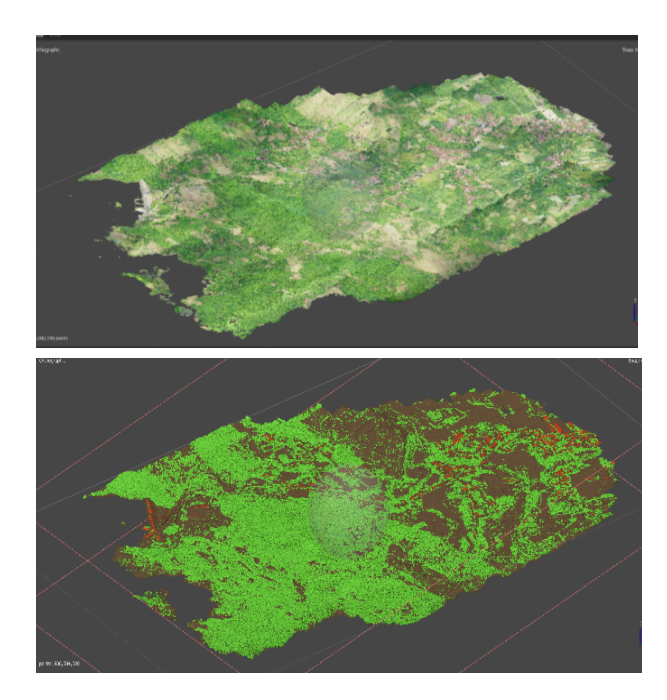


Figure 7. Build Dense Cloud & Clasify Point Cloud

Dense clouds are classified into different categories, such as land, vegetation and buildings, using both automatic and manual methods. Manual classification was performed to improve the accuracy of the results.

### **3.3.4 Build DEM**

A Digital Elevation Model (DEM) was created based on the classified ground points. The resulting DEM is a Digital Terrain Model (DTM), which is used for slope analysis. This process involves combining a number of aligned images to form an orthomosaic, which is an orthophoto image that has been geometrically corrected so that each element in it has an accurate position and is proportional to the actual conditions on the earth's surface. This orthomosaic allows for more precise spatial analysis because distortions due to camera tilt and topographic variations have been minimized. The orthomosaic results are used as a basis in land cover mapping for landslide vulnerability analysis.

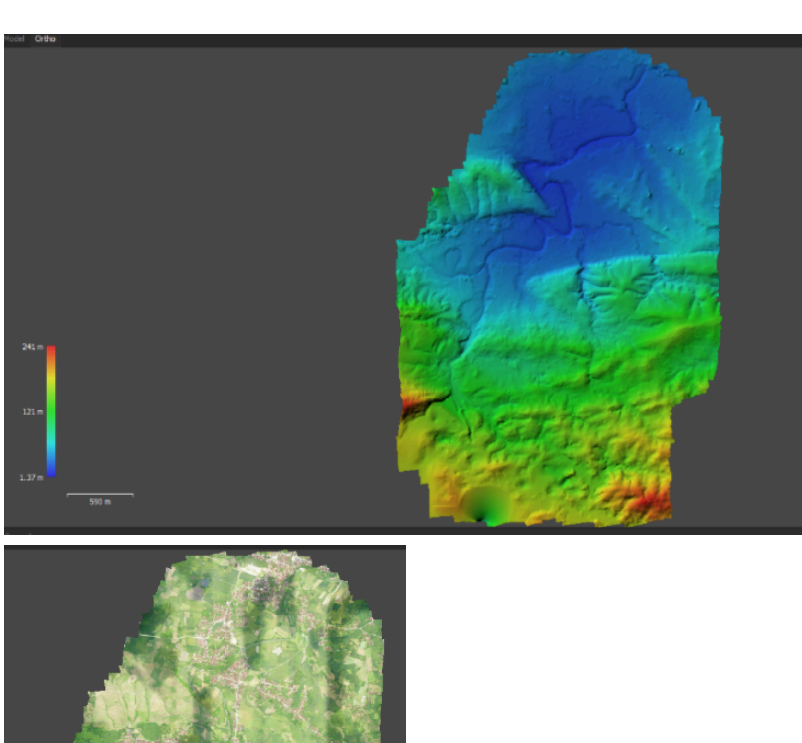


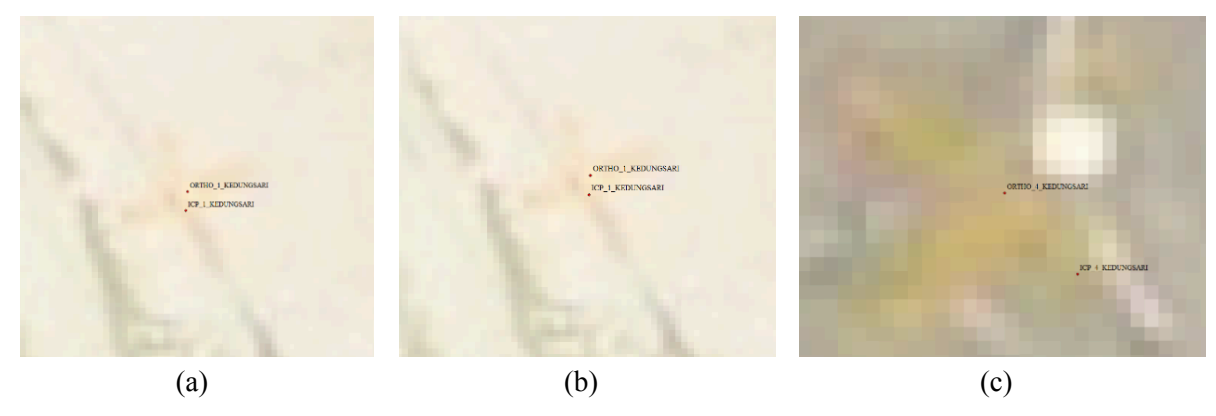


Figure 9. Build DEM and Build Orthomosaic

# 3.3.5 Orthomosaic Correction with Independent Control Point (ICP)

After the *orthomosaic* creation process from the UAV imagery was completed, spatial corrections were made using *Independent Control Points* (ICP) to improve the geometry accuracy of the mapping results. These independent control points are points that were not used in the initial georeferencing process, but were used as a validation reference for the spatial position of the *orthomosaic* results[9], [16] . By comparing the actual coordinates of the ICPs in the field and the position recorded on the map, a deviation value can be calculated which indicates the final accuracy level of the orthophoto map product. The *orthomosaic* results were corrected using *Independent* 

Control Points (ICPs). The premarks on the image are marked, and the coordinates (x, y, z) are taken to compare with the original field coordinates for horizontal and vertical correction.



**Figure 11. ICP Point Correction** 

This process ensures that the final result has high accuracy, so that it can be used in spatial analysis and more precise mapping of landslide-prone areas.

Table 3. Vertical Accuracy Test Results

NO Point Name ICP Orthophoto Mosaic Elevation (D Y) (D Y)<sup>2</sup>

NO	<b>Point Name</b>	ICP	Orthophoto Mosaic Elevation	(D Y)	$(\mathbf{D} \mathbf{Y})^2$
		Elevation			
A	В	С	D	E	F
1	ICP01	18.428	18.4051	-0.032	0.001
2	ICP02	48.896	48.3606	-0.535	0.286
3	ICP03	31.474	31.1304	-0.343	0.118
4	ICP04	117.105	116.2442	-0.860	0.740
5	ICP05	184.624	184.9935	0.369	0.136
6	ICP06	152.591	152.5868	-0.004	0.000
7	ICP07	48.510	48.506	-0.004	0.000
8	ICP08	22.079	22.0363	-0.043	0.002
9	ICP09	78.392	78.3908	-0.002	0.000
10	ICP10	84.480	84.4674	-0.013	0.000
			Total		1.283
	•	•	Average	•	0.128
			RMSE		0.358
	•	•	Accuracy	•	0.591

**Table 4. Horizontal Accuracy Test Results** 

	1001 if 1101 Editory 1000 Hoberts									
No. Poin t	Point Name	X (ICP coordinates )	X (Orthophoto Mosaic Coordinates )	DX	(D X) <sup>2</sup>	Y (ICP coordinates )	Y (Orthophoto Mosaic Coordinates )	DY	(D Y) <sup>2</sup>	(D X) <sup>2</sup> + (D Y) <sup>2</sup>
A	В	С	D	Е	F	G	Н	I	J	K
1	ICP1	134980.679	134982.696	0.017	0.000	688437.586	688437.748	0	0.026	0.027
								.162		
2	ICP2	135602.510	135602.779	0.269	0.072	687647.842	687647.842	0.000	0.000	0.072
3	ICP3	134539.205	134539.164	-0.04	0.002	687132.181	687131.838	0.343	0.118	0.119
				1						
4	ICP4	134071.388	134071.187	-0.20	0.040	686186.169	686186.447	0.278	0.077	0.118
				1						
5	ICP5	135527.596	135527.68	0.084	0.007	685661.924	685662.256	0.332	0.110	0.117
6	ICP6	134935.834	134935.837	0.003	0.000	685709.854	685709.909	0.055	0.003	0.003
7	ICP7	135753.618	135753.449	-0.11	0.014	687306.294	687306.235	0.059	0.003	0.018
				9						
8	ICP8	135243.742	135243.678	-0.06	0.004	688162.051	688162.209	0.158	0.025	0.029
				1						

9	ICP9	134008.063	134008.084	0.021	0.000	687901.076	687901.206	0.130	0.017	0.017
 10	ICP10	135113.350	135113.352	0.002	0.000	686567.521	686567.609	0.088	0.008	0.008
				To	tal					0.528
				Avei	rage					0.053
RMSE							0.230			
,		•	•	Accu	racy	•	•			0.349

The accuracy assessment in this study yielded a Root Mean Square Error (RMSE) of 0.230 meters. Compared to global standards, this value falls within the high-precision category and exceeds the minimum thresholds set by both ASPRS Class 1 ( $\leq$  0.15 meters) and USGS Quality Level 2 ( $\leq$  0.20 meters). Although slightly above the ASPRS Class 1 threshold, the accuracy achieved is significantly superior to that of global DEM products such as TanDEM-X, which typically has an average RMSE of  $\pm$ 2 meters, and SRTM, with RMSE values ranging from  $\pm$ 6 to  $\pm$ 16 meters depending on topography. Furthermore, according to the Indonesian Geospatial Information Agency (BIG), the national DEM (DEMNAS) has an average vertical RMSE of approximately  $\pm$ 2.5 meters. Therefore, the RMSE of 0.230 meters achieved in this study demonstrates a substantially higher level of accuracy compared to both national and global DEM standards.

# 3.4. Land Slope Classification

Topography is defined as the elevation condition of a location and the level of its slope[15]. In Kedungsari Village the terrain presents an uneven patchwork that shifts abruptly from level fields to sharply inclined ridges. The current survey relied on a Digital Terrain Model compiled from drone-acquired images; those data were subsequently sorted by both elevation and gradient. The sorting exercise produced five distinct slope categories:

Table 5. Slope Classification							
NO Classification Slope (%)							
1	Flat	0 - 8					
2	Ramps	8 - 15					
3	Medium	15 - 30					
4	Steep	30 - 45					
5	Very steep	>45					

The classification results show that most of Kedungsari Village has a fairly high slope, especially in the southern part of the village which is a forest area.

Classification is done in two main stages:

- 1. Calculating Slope
  - Using the *Slope Tool* to calculate the slope level based on DEM data.
  - Slope is measured in percentage (%), so that the results are suitable for subsequent classification analysis.
- 2. Reclassify
  - The rasterized results of Slope were then *reclassified* into five slope categories using the *Reclassify Tool*.

This process aims to identify areas with slope levels that are at high risk of landslides, so that it can be used as a basis in analyzing landslide vulnerability in Kedungsari Village.

### 3.5. Results of Land Slope Classification

This research utilizes *Unmanned Aerial Vehicle* (UAV)-based photogrammetry technology to produce a *digital elevation* model (DEM) as the basis for spatial analysis of land slope in Kedungsari Village. This analysis has the main objective to identify areas with high slope levels and potential landslide-prone zones. Based on the results of the interpretation and processing of drone image data in

2024, spatial information was obtained showing variations in land slope levels classified into five categories, namely: <20%, 20-40%, 40-60%, 60-80%, and >80%.

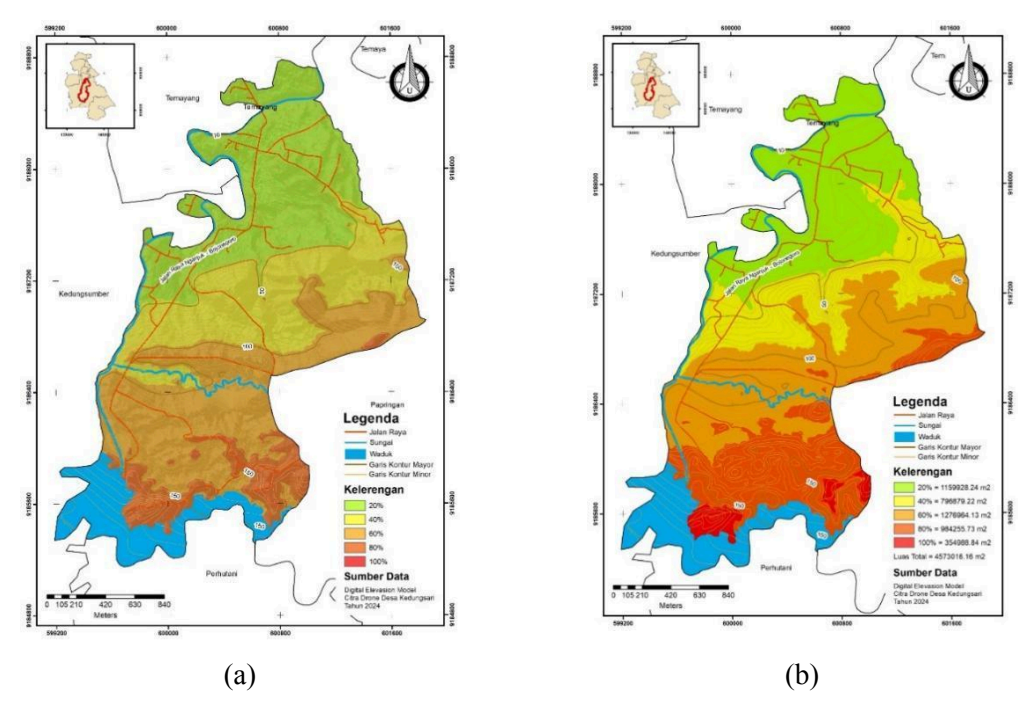


Figure 4. (a) Slope Map, (b) Slope Map With Area

The map of slope classification results (Figure a) shows that the distribution of areas with high slopes, particularly above 60%, is concentrated in the southern and southwestern parts of Kedungsari Village, which includes state forest areas (Perhutani). The land area with 60% slope reaches 1,276,964.13 m<sup>2</sup>, while 80% and 100% slope cover 984,255.73 m<sup>2</sup> and 354,988.84 m<sup>2</sup> respectively. Combined, areas with slopes greater than 60% cover about 2.6 million m<sup>2</sup> of the total area of 4.573.016.16 m<sup>2</sup>, which means nearly 57% of the village area is vulnerable to land mass movements. especially when affected by heavy rainfall or human activities. Numerous studies have shown that very steep slopes (>60%) have a high level of vulnerability to landslide events, especially when influenced by high intensity rainfall [19], [20]. In addition, human interventions such as excavation and land use changes exacerbate slope instability, thereby increasing the potential for ground motion[21], [22]. (Figure b) reinforces the classification results with a more detailed visualization of the spatial distribution of slope, showing the undulating topography in the south and southwest areas categorized as very steep zones. These areas are characterized by orange to dark red color gradations, indicating high levels of slope steepness. Meanwhile, the northern and eastern areas of the village are dominated by low to moderate slopes (<40%), which are characterized by green and yellow colors on the map.

Figure 5. RTRW Map

The slope mapping results using UAV indicate that approximately 57% of Kedungsari Village has a slope gradient exceeding 40%, with the dominant classifications falling into the steep (30–45%) and very steep (>45%) categories. In contrast, the slope map from the Bojonegoro Regency Spatial Plan (RTRW) generally classifies the area as having moderate to steep slopes, without clear delineation of zone boundaries or spatial variability. In the southern and southwestern parts of the village, the UAV-based map identifies several pockets of extreme slopes (>60%) that are not specifically represented in the RTRW map. This highlights the UAV-derived map's capability to capture micro-topographic contours and local elevation variations in greater detail.

This finding is crucial in the context of disaster mitigation, as high slope distribution is directly correlated with landslide potential. Therefore, the results of this analysis can be used as an initial reference in the preparation of a landslide vulnerability zoning map as well as a consideration in land use planning and environmental management in Kedungsari Village in a sustainable manner.

### 4. Conclusion

This research shows that the utilization of unmanned aircraft (UAV)-based photogrammetric technology provides effective results in obtaining high-quality topographic data for the Kedungsari Village area. Through a series of processes, ranging from aerial image acquisition, determination of control points using geodetic GPS, to digital surface modeling and spatial analysis, detailed and reliable land slope information is obtained. The mapping results show that the distribution of land slope in Kedungsari Village varies widely, with a concentration of steep to very steep areas (>60%) dominantly located in the southern and southwestern parts of the village. These high slope areas account for more than half of the total area, making them a high-risk zone for potential landslides, especially during the rainy season or due to human activities that destabilize the slopes. Thus, the UAV mapping approach not only provides efficiency in the field survey process, but also produces spatial products that have high accuracy and are relevant for disaster mitigation analysis needs. The results of this research are expected to be used as a reference in the preparation of landslide-prone zoning maps.

# Reference

[1] F. Dadrass Javan, F. Samadzadegan, A. Toosi, and M. van der Meijde, "Unmanned Aerial Geophysical Remote Sensing: A Systematic Review," *Remote Sens.*, vol. 17, no. 1, 2025, doi: 10.3390/rs17010110.

- [2] D. C. Tsouros, S. Bibi, and P. G. Sarigiannidis, "A review on UAV-based applications for precision agriculture," *Inf.*, vol. 10, no. 11, 2019, doi: 10.3390/info10110349.
- [3] F. Mancini, M. Dubbini, M. Gattelli, F. Stecchi, S. Fabbri, and G. Gabbianelli, "Using unmanned aerial vehicles (UAV) for high-resolution reconstruction of topography: The structure from motion approach on coastal environments," *Remote Sens.*, vol. 5, no. 12, pp. 6880–6898, 2013, doi: 10.3390/rs5126880.
- [4] F. Pessacg *et al.*, "Simplifying UAV-Based Photogrammetry in Forestry: How to Generate Accurate Digital Terrain Model and Assess Flight Mission Settings," *Forests*, vol. 13, no. 2, pp. 1–27, 2022, doi: 10.3390/f13020173.
- [5] D. H. Rachmanto and M. Ihsan, "Pemanfaatan Metode Fotogrametri Untuk Pemetaan Skala 1: 1000 (Studi Kasus: Universitas Pendidikan Indonesia)," *J. ENMAP*., vol. 1, no. 2, pp. 81–86, 2020, doi: 10.23887/em.v1i2.28173.
- [6] S. J. Sutanto and B. W. Ridwan, "Teknologi Drone Untuk Pembuatan Peta Kontur: Studi Kasus Pada Kawasan P3Son Hambalang," *J. Tek. Hidraul.*, vol. 7, no. 2, pp. 179–194, 2016.
- [7] J. Grau *et al.*, "Using unmanned aerial vehicle and lidar-derived dems to estimate channels of small tributary streams," *Remote Sens.*, vol. 13, no. 17, 2021, doi: 10.3390/rs13173380.
- [8] M. Uysal, A. S. Toprak, and N. Polat, "DEM generation with UAV Photogrammetry and accuracy analysis in Sahitler hill," *Meas. J. Int. Meas. Confed.*, vol. 73, pp. 539–543, 2015, doi: 10.1016/j.measurement.2015.06.010.
- [9] X. Liu, X. Lian, W. Yang, F. Wang, Y. Han, and Y. Zhang, "Accuracy Assessment of a UAV Direct Georeferencing Method and Impact of the Configuration of Ground Control Points," *Drones*, vol. 6, no. 2, 2022, doi: 10.3390/drones6020030.
- [10] K. Zhang, H. Okazawa, K. Hayashi, T. Hayashi, L. Fiwa, and S. Maskey, "Optimization of Ground Control Point Distribution for Unmanned Aerial Vehicle Photogrammetry for Inaccessible Fields," *Sustain.*, vol. 14, no. 15, 2022, doi: 10.3390/su14159505.
- [11] B. Awasthi, S. Karki, P. Regmi, D. S. Dhami, S. Thapa, and U. S. Panday, "Analyzing the effect of distribution pattern and number of GCPs on overall accuracy of UAV photogrammetric results," *Lect. Notes Civ. Eng.*, vol. 51, no. November 2020, pp. 339–354, 2020, doi: 10.1007/978-3-030-37393-1 29.
- [12] D. L. Elian, "ANALISA BIAYA, MUTU, DAN WAKTU PENGAMBILAN DATA TOPOGRAFI MENGGUNAKAN METODE TERESTRIS DAN DRONE MAPPING atau UAV (Unmanned Aerial Vehicle)," *J. Inform. dan Tek. Elektro Terap.*, vol. 9, no. 3, pp. 86–89, 2021, doi: 10.23960/jitet.v9i3.2433.
- [13] M. A. Setiawan, E. B. Wahyono, and B. Suyudi, "Hasil Pemotretan Unmanned Aerial Vehicle Pada Variasi Topografi Untuk Pengukuran dan Pemetaan," *Tunas Agrar.*, vol. 2, no. 1, pp. 21–44, 2019, doi: 10.31292/jta.v2i1.16.
- [14] A. T. Sutjipto, T. T. Purwiyono, and M. A. Azizi, "Monitoring Pergerakan Massa Batuan Dengan Metode Terestris Menggunakan Total Station Dan Metode Fotogrametri Di Kaliwadas, Kebumen, Jawa Tengah," *Proceeding Semin. Nas. Geomekanika IV Padang*, no. October, pp. 225–231, 2017.
- [15] S. N. Husna, S. Subianto, and Hani'ah, "Penggunaan Parameter Orientasi Eksternal (eo) Untuk Optimlisasi Digital Triangulasi Fotogrametri Untuk Keperluan Ortofoto," vol. 5, pp. 188–195, 2016
- [16] M. V. Y. Garcia and H. C. Oliveira, "The Influence of Ground Control Points Configuration and Camera Calibration for Dtm and Orthomosaic Generation Using Imagery Obtained from A Low-Cost Uav," *ISPRS Ann. Photogramm. Remote Sens. Spat. Inf. Sci.*, vol. 5, no. 1, pp. 239–244, 2020, doi: 10.5194/isprs-annals-V-1-2020-239-2020.
- [17] and N. S. Thomas R. Chudley1, Poul Christoffersen1, Samuel H. Doyle2, Antonio Abellan3, "High-accuracy UAV photogrammetry of ice sheet dynamics with no ground control," 2011.
- [18] S. I. Jiménez-Jiménez, W. Ojeda-Bustamante, M. D. J. Marcial-Pablo, and J. Enciso, "Digital terrain models generated with low-cost UAV photogrammetry: Methodology and accuracy," *ISPRS Int. J. Geo-Information*, vol. 10, no. 5, 2021, doi: 10.3390/ijgi10050285.
- [19] M. Miftakhul Huda, M. Zainul Ikhwan, and M. Insan Rendra, "Pendekatan Analisis Spasial

- untuk Deteksi Kerawanan Longsor di Kecamatan Kedungadem Kabupaten Bojonegoro," *Inf. (Jurnal Inform. dan Sist. Informasi)*, vol. 16, no. 1, pp. 98–119, 2024, doi: 10.37424/informasi.v16i1.297.
- [20] D. Kurniawati, I. Meviana, and N. luky Setyowati, "Identifikasi Karakteristik Dan Faktor Pengaruh Pada Bencana Longsor Lahan Di Kecamatan Dau," *J. SWARNABHUMI J. Geogr. dan Pembelajaran Geogr.*, vol. 7, no. 2, pp. 142–149, 2022, doi: 10.31851/swarnabhumi.v7i2.7686.
- [21] D. Sarah *et al.*, "Back Analysis of Rainfall-Induced Landslide in Cimanggung District of Sumedang Regency in West Java Using Deterministic and Probabilistic Analyses," pp. 1–22, 2024.
- [22] Q. Lan, J. Tang, X. Mei, X. Yang, Q. Liu, and Q. Xu, "Hazard Assessment of Rainfall–Induced Landslide Considering the Synergistic Effect of Natural Factors and Human Activities," *Sustain.*, vol. 15, no. 9, 2023, doi: 10.3390/su15097699.

### How to cite this article:

Mrabawani Insan Rendra. Integration of UAV Photogrammetry and GIS in High-Resolution Topographic Mapping of Kedungsari Village, Temayang Subdistrict. *Jurnal Teknologi dan Manajemen*. 2025 July; 6(2):109-124. DOI: 10.31284/j.jtm.2025.v6i2.7849